교육학석사 학위논문

Ferroelectric Stability and Switching Kinetics of $Hf_{0.5}Zr_{0.5}O_2$ Under ^{60}Co Gamma-ray Irradiation

^{60}Co 감마선 조사에 의한 $Hf_{0.5}Zr_{0.5}O_2$ 강유전 안정성과 스위칭 동역학 분석

2022년 2월

서울대학교 대학원

과학교육과 물리 전공

남궁진

Ferroelectric Stability and Switching Kinetics of $Hf_{0.5}Zr_{0.5}O_2$ Under ^{60}Co Gamma-ray Irradiation

지도교수 채 승 철

이 논문을 교육학석사 학위논문으로 제출함
2022년 2월

서울대학교 대학원
과학교육과 물리 전공
남 궁 진

남궁진의 석사 학위논문을 인준함
2022년 2월

위 원 장 조 정 효 (인)

부위원장 채 승 철 (인)

위 원 전 동 렬 (인)

Abstract

We report the effect of ^{60}Co gamma-ray irradiation on the ferroelectric properties of metal-ferroelectric $Hf_{0.5}Zr_{0.5}O_2$-metal thin film structures. The pristine $Hf_{0.5}Zr_{0.5}O_2$ films showed strong radiation tolerance against gamma-rays with stable remnant polarization values. When $Hf_{0.5}Zr_{0.5}O_2$ films were exposed to electric field cycling, or ‘wake-up’ process, prior to irradiation, however, their ferroelectricity demonstrated a clear degradation of remnant polarization and coercive voltage shift of the hysteresis curves. The analysis of ferroelectric switching dynamics revealed faster polarization switching with broadening of Lorentzian distribution of characteristic switching time for higher radiation doses, which is contrary to the wake-up behavior. The relationship between the wake-up process and gamma-ray irradiation on the stability of ferroelectric $Hf_{0.5}Zr_{0.5}O_2$ films was discussed in light of domain alignment and defect mechanisms, considering both the redistribution and trapping of defect charges.

Keyword : Ferroelectricity, $Hf_{0.5}Zr_{0.5}O_2$, gamma-ray, wake-up, switching dynamics, defect
Student Number : 2020-27908

Table of Contents

Abstract ……..i

Table of Contents ……..ii

List of Figures ……..iii

I. Introduction ……...1

II. Material and Methods ……3

III. Results and Discussion ……...4

3.1. Pristine $Hf_{0.5}Zr_{0.5}O_2$ ……4

3.2. Woken-up $Hf_{0.5}Zr_{0.5}O_2$ ……6

3.3. Switching Dynamics of $Hf_{0.5}Zr_{0.5}O_2$ ……8

3.4. The Effect of Radiation-induced Defects ……...11

IV. Conclusion ……15

References ……...16

Abstract in Korean ……22

List of Figures

Fig. 1. Experimental schematics of the time diagram with electrical measurements and the wake-up process (a) excluding irradiation (b) including irradiation before electrical measurements and the wake-up process. (c)-(d) The results of polarization-voltage and current-voltage hysteresis measurements for pristine and woken-up cells in the nonirradiated and 1 Mrad irradiated conditions. (e) Dielectric constant values calculated from capacitance-voltage measurements. (f) Values of remnant polarization for both pristine and woken-up cells with respect to total radiation dose.....5

Fig. 2. Experimental schematics of the time diagram with the wake-up process and electrical measurement (a) excluding irradiation (b) including irradiation between the wake-up process and electrical measurements (c) including irradiation followed by an additional wake-up process. (d)-(e) The results of polarization-voltage and current-voltage hysteresis measurements for the three cases depicted in (a)-(c) with a total radiation dose of 1 Mrad. (f)-(g) Values of coercive voltage shift and remnant polarization values derived from polarization-voltage hysteresis measurements with respect to total radiation dose. 7

Fig. 3. Ferroelectric switching dynamics of $Hf_{0.5}Zr_{0.5}O_2$ thin films after the rewake-up process. (a)-(c) Time dependence of the ratio of polarization flipping, $\Delta P(t)$, with various write pulse widths and pulse amplitudes from 1.8 V to 3.0 V in 0.3 V intervals for different amounts of total radiation dose. (d)-(f) Lorentzian distribution function $F(\log(t_0))$ from fitting of switching dynamics based on the Lorentzian distribution of logarithmic switching time for different radiation doses. (g)-(i) Comparisons of the Lorentzian distribution function $F(\log(t_0))$ for different total radiation doses with respect to the external voltage. 10

Fig. 4. Schematics describing the effects of defects on the Lorentzian distribution function of switching time. (a) Variation in the characteristic switching time and location of the distribution function based on the role of defects as nucleation sites or domain-wall pinning sites. (b) Variation of broadness of distribution function due to induced local field by defects. 14

I. Introduction

The unprecedented ferroelectricity in hafnium oxide reported since 2011 has attracted attention for its potential applications in various technological devices [1-5]. Despite the limitations which prevent the use of perovskite ferroelectric materials, such as $PbZr_{1-x}Ti_xO_3$ and $BaTiO_3$, in practical applications at modern process node widths [6], hafnium oxides are still given serious consideration for use in memory devices, such as ferroelectric random access memory (FeRAM) and ferroelectric field-effect transistor (FeFET), due to their scalable advantages, non-volatile properties, and strong CMOS compatibility [7]. Robust ferroelectricity of remarkably ultrathin (thickness of under 2 nm) $Hf_{0.8}Zr_{0.2}O_2$ has been achieved without requiring a 'wake-up' effect [8]. Si-doped HfO_2 was successfully integrated into FeFET devices and realized with 28 nm high-k metal gate (HKMG) CMOS technology [9]. Furthermore, due to the intriguing stability of individual ferroelectric dipole moments based on the flat ferroelectric phonon band, ferroelectric HfO_2 is considered to have potential uses in ultrahigh-density memory devices with atomic-scale operationality [10].

Considering the diverse hafnium-based ferroelectric memory applications in a wide range of fields, including high radiation environments such as nuclear power plants and outer space, an investigation of the radiation tolerance of $Hf_{0.5}Zr_{0.5}O_2$ films is required prior to industrial application. Sun et al. asserted that ferroelectric $Hf_{1-x}Zr_xO_2$ thin film capacitors have great potential for application to FeRAM in radiation environments [11]. Moreover, Zhang et al. reported that Zr and Al-doped HfO_2 films also show radiation tolerance, further supporting their use in forward-

looking applications [12]. On the other hand, hafnium zirconium oxide-based FeFETs in the gate stack configuration were reported to have degradation of ferroelectricity due to radiation-induced oxygen vacancies and lattice distortion [13]. Additionally, it is widely known that electron-hole pairs are generated when high-energy radiation, such as gamma-rays, influences the oxide layer leading to disadvantageous operation of devices due to trapping of electrons and holes [13, 14]. Oxygen vacancies are generated due to irradiation because the atomic ratio of Hf to O increases after gamma-ray irradiation [15]. Given the disagreement reported in prior studies regarding the overall effect of irradiation on hafnium-based ferroelectric materials, more detailed research is necessary to determine how radiation-induced defects influence their basic ferroelectric characteristics and switching kinetics under practical use.

In the present study, we investigated the response of ferroelectric $Hf_{0.5}Zr_{0.5}O_2$ films to gamma-ray irradiation under different external electric stimuli. The film stoichiometry for gamma-ray irradiation was evaluated with respect to the strong and stable ferroelectricity of $Hf_{0.5}Zr_{0.5}O_2$ [16]. A strong radiation tolerance was observed in the pristine specimen, whereas the specimen exposed to external field cycling, known as a ‘wake-up’ process, before gamma-ray irradiation exhibited significant changes in ferroelectric switching dynamics as well as static ferroelectric properties. Given this conditional gamma-ray tolerance, the relationship between the wake-up effects and defect generation by gamma-ray irradiation was discussed, specifically focusing on the redistribution of charged defects related to wake-up status and trapping and detrapping of charged defects.

II. Material and Methods

Conventional metal-ferroelectric-metal (MFM) capacitor structures of the $Hf_{0.5}Zr_{0.5}O_2$ ferroelectric layer were prepared by using the atomic layer deposition (ALD) method with tetrakis (ethylmethylamido) hafnium (TEMAH), tetrakis (ethylmethylamido) zirconium (TEMAZ), and ozone. Ten nanometer thick $Hf_{0.5}Zr_{0.5}O_2$ films were grown at 280 ℃, and titanium nitride (TiN) electrodes were deposited at bottom and top by DC sputtering. Subsequently, the films were postannealed at 600 °C for 30 seconds in a N_2 environment to create a ferroelectric phase. The polarization-voltage (P-V) hysteresis and switching dynamics were measured with a semiconductor parameter analyzer (Model 4200-SCS, Keithley) and ferroelectric tester (TF Analyzer 3000, aixACCT). All electrical field cycling conditions for the 'wake-up' process were carried out with 10^5 pulses at 3 V. The capacitance-voltage (C-V) measurements were performed with an impedance analyzer (Model E4990A, Keysight). The $Hf_{0.5}Zr_{0.5}O_2$ MFM capacitors were irradiated via ^{60}Co gamma-rays at the Advanced Radiation Technology Institute (ARTI, an affiliate of the Korea Atomic Energy Research Institute).

III. Results and Discussion

3.1. Pristine $Hf_{0.5}Zr_{0.5}O_2$

The pristine $Hf_{0.5}Zr_{0.5}O_2$ thin films exhibited strong irradiation tolerance against gamma-rays. Variation in ferroelectric properties of the $Hf_{0.5}Zr_{0.5}O_2$ film after irradiation with gamma-rays were investigated prior to any electrical measurement to determine the overall effect of irradiation on the specimen. Figures 1(a) and 1(b) show simplified schematics of experimental electrical measurement sequences with gamma-ray irradiation. Following the schematic procedure, the P-V hysteresis and current-voltage characteristics of pristine and electrically stimulated, i.e., woken-up, cells show negligible differences between irradiated and nonirradiated cells, as shown in Figs. 1(c) and 1(d), respectively. The remnant polarization values after the wake-up process for nonirradiated and 1 Mrad irradiated films are 17.7 and 17.6 $\mu C/cm^2$, respectively, as shown in Fig. 1(c). The ferroelectric switching current shows little difference for non-irradiated and 1 Mrad irradiated films, each of which shows the enhancement of the current peak only after the wake-up process, as shown in Fig. 1(d). In addition, the tolerance of gamma-ray irradiation to ferroelectric hysteresis loops was maintained for the total radiation dose ranging from 1 to 10 Mrad. Radiation irrelevance was also observed in the capacitance-voltage measurement, as shown in Fig. 1(e). As for the remnant polarization values (P_r), the radiation irrelevance of the $Hf_{0.5}Zr_{0.5}O_2$ film was relatively well conserved at different radiation doses, as shown in Fig. 1(f). The enhanced remnant polarization values, when the wake-up process followed irradiation, were between 6.8 and 7.0 $\mu C/cm^2$ for all cases.

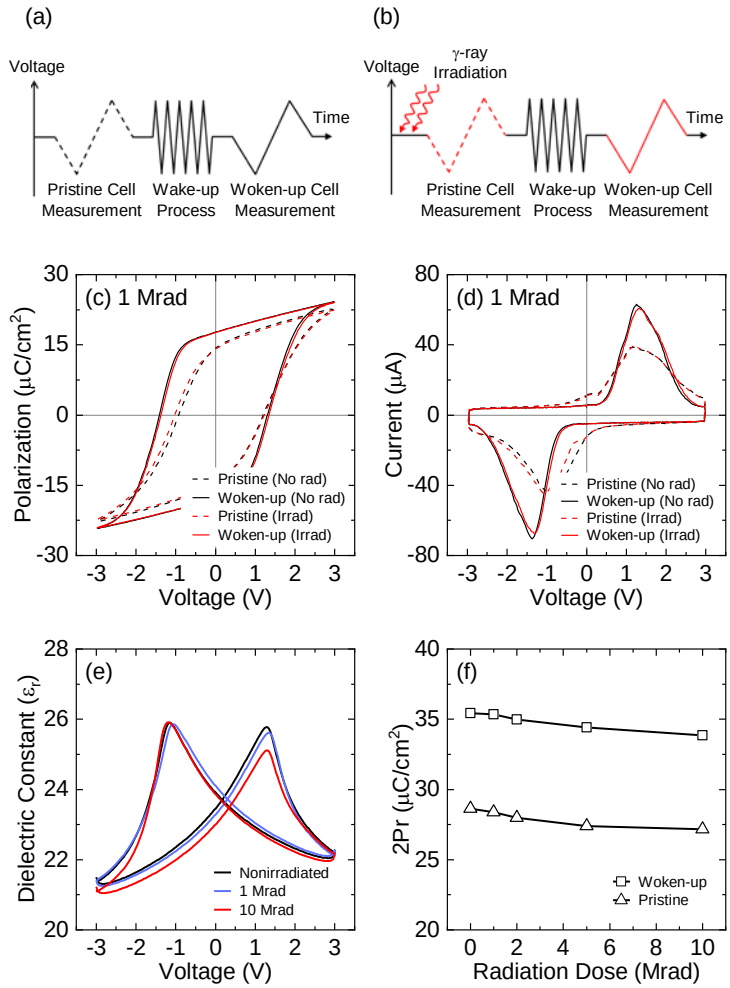

Fig. 1. Experimental schematics of the time diagram with electrical measurements and the wake-up process (a) excluding irradiation (b) including irradiation before electrical measurements and the wake-up process. (c)-(d) The results of polarization-voltage and current-voltage hysteresis measurements for pristine and woken-up cells in the nonirradiated and 1 Mrad irradiated conditions. (e) Dielectric constant values calculated from capacitance-voltage measurements. (f) Values of remnant polarization for both pristine and woken-up cells with respect to total radiation dose.

3.2. Woken-up $Hf_{0.5}Zr_{0.5}O_2$

In contrast, when gamma-ray irradiation was induced after the wake-up process, clear ferroelectric degradation was observed in the $Hf_{0.5}Zr_{0.5}O_2$ thin film. The effect of gamma-ray irradiation on the woken-up specimen was also investigated in terms of the variation in $Hf_{0.5}Zr_{0.5}O_2$ ferroelectric properties after irradiation with gamma-rays. Figures 2(a)-(c) show the simplified schematics of experimental electrical measurement sequences, including gamma-ray irradiation and the wake-up process. To compare the irradiation effect after the wake-up process, gamma-ray irradiation was conducted after electric field cycling, as shown in Fig. 2(b). The additional electric field cycling was conducted to investigate the overall change in the characteristics induced by gamma-ray irradiation, as shown in Fig. 2(c). The P-V hysteresis and current-voltage shapes of the woken-up specimen exhibited degradation of the remnant ferroelectric polarization, from 18.3 $\mu C/cm^2$ to 15.1 $\mu C/cm^2$ after gamma-ray irradiation, and a shift toward negative voltage, depicted with solid red lines in Figs. 2(d) and 2(e). The subsequent wake-up process after irradiation partly restored the remnant polarization value, and the overall shape of the ferroelectric switching current resembled the wake-up behavior in hysteresis and switching current, depicted with solid blue lines in Figs. 2(d) and 2(e), respectively. The overall results of the coercive voltage (V_C) shift and suppressed $2P_r$ values with respect to gamma-ray radiation dose are shown in Figs. 2(f) and 2(g). Identical electric stimulus conditions of the rewake-up process lead to the restoration of symmetric hysteresis loops in the coercive voltage (V_C) shifts by the redistribution of asymmetrically trapped charge defects [17]. However, the specimens still show degraded polarization in Fig. 2(g).

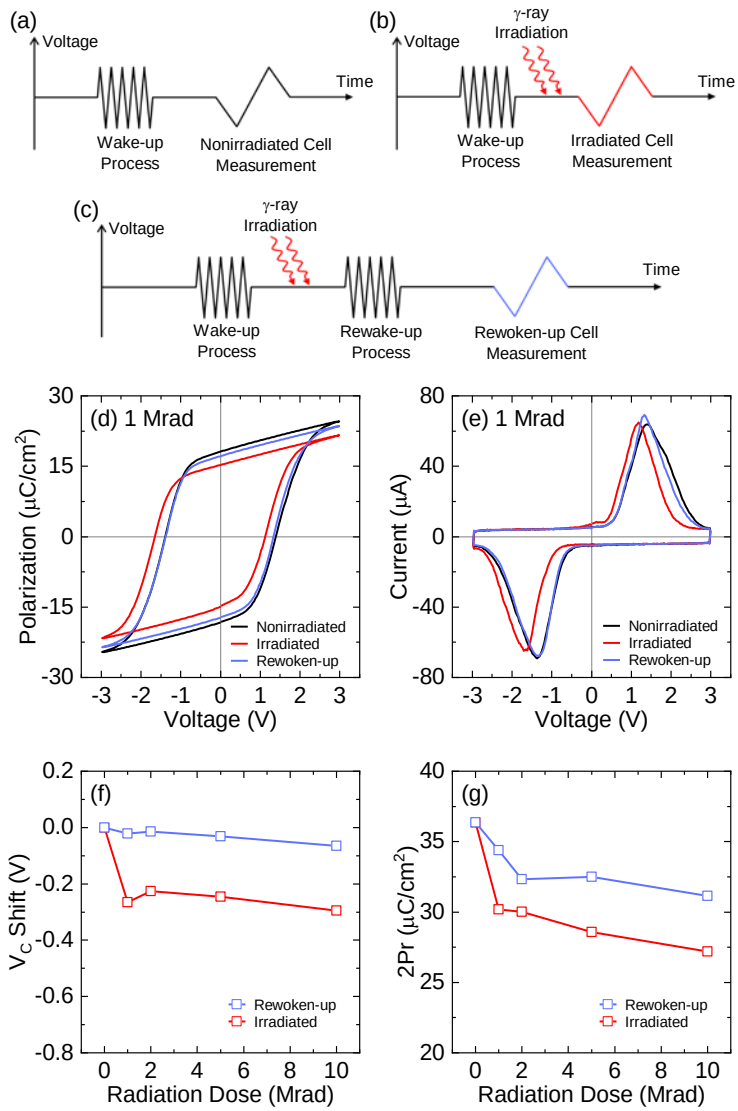

Fig. 2. Experimental schematics of the time diagram with the wake-up process and electrical measurement (a) excluding irradiation (b) including irradiation between the wake-up process and electrical measurements (c) including irradiation followed by an additional wake-up process. (d)-(e) The results of polarization-voltage and current-voltage hysteresis measurements for the three cases depicted in (a)-(c) with a total radiation dose of 1 Mrad. (f)-(g) Values of coercive voltage shift and remnant polarization values derived from polarization-voltage hysteresis measurements with respect to total radiation dose.

3.3. Switching Dynamics of $Hf_{0.5}Zr_{0.5}O_2$

The dynamics of ferroelectric switching were investigated to unveil the conditional effect of gamma-ray irradiation on the ferroelectricity of the $Hf_{0.5}Zr_{0.5}O_2$ thin film. A positive electric pulse of 3 V height and 125 μs width was applied at the top electrode to induce full saturation of ferroelectric polarization, and the portion of switched polarization was measured by introducing a negative pulse to the top electrode. The negative pulse width and height were subsequently increased to estimate the time evolution of polarization switching given as $\Delta P(t)/2P_s$. Figures 3(a)-(c) demonstrate the time and voltage dependences of ferroelectric polarization in the $Hf_{0.5}Zr_{0.5}O_2$ thin film for the nonirradiated, 1 Mrad irradiated, and 10 Mrad irradiated films, respectively, after electric field cycling on the pristine specimens; the empty symbols represent the value of polarization switching from the experiment with different applied voltages ranging from 1.8 to 3.0 V in 0.3 V intervals. Clear polarization reversal along the external electric bias was observed in all the specimens. As the external bias was increased above the coercive voltage, a steep reversal of polarization was obtained, whereas gradual polarization reversal was observed in the low bias cases.

The analysis of ferroelectric switching dynamics in terms of the switching time demonstrated the effect of gamma-ray irradiation on the ferroelectric properties. Transient polarization reversals were analyzed based on the nucleation limited switching (NLS) model, which is known as a common mechanism for the reversal of order parameters with disorders [18, 19]. The solid lines in Figs. 3(a)-(c) represent the fitting results obtained from the NLS model, with a Lorentzian distribution for the switching time as follows:

$$\frac{\Delta P(t)}{2P_s} = \int_{-\infty}^{\infty} \left[1 - \exp\left\{-\left(\frac{t}{t_0}\right)^2\right\}\right] F(\log t_0) d(\log t_0),$$

where

$$F(\log t_0) = \frac{A}{\pi}\left[\frac{w}{(\log t_0 - \log t_1)^2 + w^2}\right],$$

and $A, w,$ and $\log t_1$ indicate a normalization constant, the half-width at half-maximum of the distribution, and the mean value of the distribution, respectively [19, 20]. Figures 3(d)-(f) show the extracted Lorentzian distribution of switching time from the analysis shown in Figs. 3(a)-(c).

Interestingly, gamma-ray irradiation shows clear broadening of the distribution of the switching time as the dose amount increases. Figures 3(g)-(i) show the Lorentzian distribution of switching time with external biases of 3.0, 2.7, and 2.4 V, respectively. Each distribution was compared with different gamma-ray doses, i.e., nonirradiated, 1 Mrad, and 10 Mrad. As shown in Figs. 3(g)-(i), the half-width at half-maximum of each distribution was broadened, and the main peak position shifted toward lower logarithmic time. Even though the virgin $Hf_{0.5}Zr_{0.5}O_2$ films showed robust gamma-ray tolerance, the specimens exposed to external electric field cycling exhibited clear polarization degradation and a broadened distribution function with decreasing characteristic switching time.

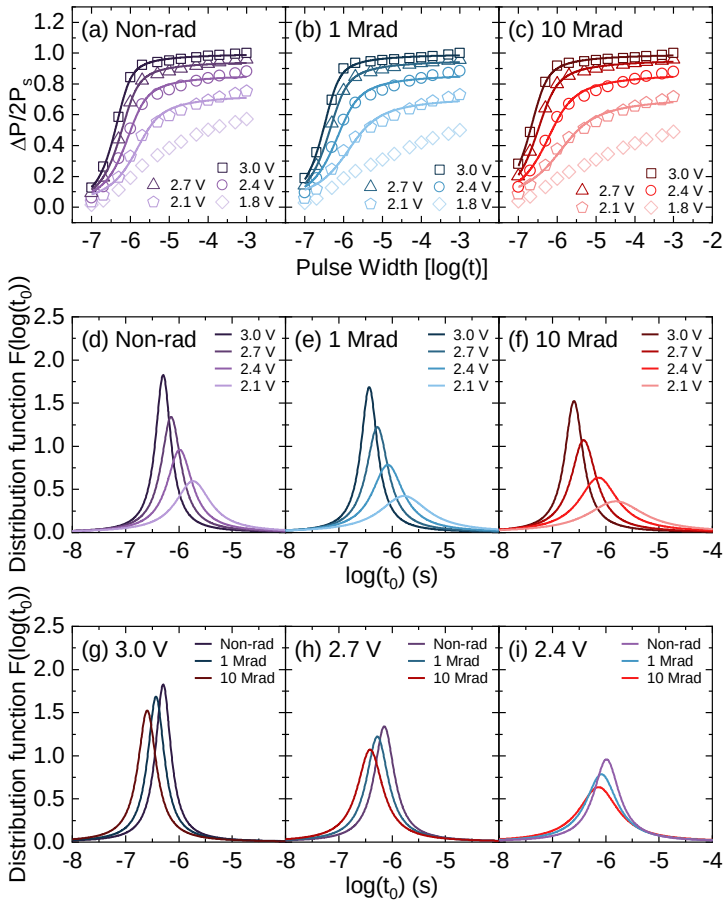

Fig. 3. Ferroelectric switching dynamics of $Hf_{0.5}Zr_{0.5}O_2$ thin films after the rewake-up process. (a)-(c) Time dependence of the ratio of polarization flipping, $\Delta P(t)$, with various write pulse widths and pulse amplitudes from 1.8 V to 3.0 V in 0.3 V intervals for different amounts of total radiation dose. (d)-(f) Lorentzian distribution function $F(\log(t_0))$ from fitting of switching dynamics based on the Lorentzian distribution of logarithmic switching time for different radiation doses. (g)-(i) Comparisons of the Lorentzian distribution function $F(\log(t_0))$ for different total radiation doses with respect to the external voltage.

3.4. The Effect of Radiation-induced Defects

The broadening of the distribution coincident with the shift toward a lower logarithmic time simultaneously indicates that the robustness of the ferroelectric polarization weakens with gamma-ray irradiation. The mechanism of nucleation and domain growth has been considered the key parameter determining the feature of switching kinetics. Due to the existence of defects in the ferroelectric layer or interfaces between the ferroelectric layer and electrode, it is possible to lower the energy barrier for nucleation at defect sites and cause ferroelectric switching to occur [21]. Additionally, it is well known that defects can also pin domain walls and prevent sideways growth [22, 23]. The change in the sharpness of the distribution function and peak position associated with the variation in the switching mechanism has been analyzed in terms of these oxide defects that induce local fields and nucleation sites for various ferroelectric oxide films [19, 24]. Since nucleation precedes domain growth in ferroelectric switching, the lower characteristic switching time for a higher radiation dose can be explained by more radiation-induced defects generating nucleation sites, following the red line in Fig. 4(a). Moreover, nucleation for polarization switching occurs inhomogeneously if defects are present [21]. The inhomogeneity could be explained by either different energy barriers for nucleation depending on defect sites or by defect-induced local electric fields, which would lead to unsynchronized switching and broadened Lorentzian distribution of switching time, as shown in Fig. 4(b). Therefore, the results of the broadening distribution function with respect to radiation dose suggest that more defects are generated by higher radiation energy.

The radiation influence on the chemical structure of the HfO_2 films has also

been investigated in terms of the formation of oxygen vacancies and subsequent chemical/electrical reactions. A dominant defect is characterized as oxygen vacancies with trap charge densities on the order of 10^{11}-10^{12} cm^{-2} [15, 25]. These trap charges induce a change in the electrical properties of the device, e.g., a shift in the capacitance-voltage curves [26]. The subsequent electron-hole pairs generated from radiation and their dissociation have been shown to affect charge transport properties [27]. The radiation tolerance of HfO_2 was reported to be weaker than that of other perovskite materials, such as $LaAlO_3$, $NdAlO_3$, and SiO_2 [28]. The inevitable oxygen vacancies in ferroelectric HfO_2 could be formed in the film before any electric measurements. However, conventional polarization-voltage hysteresis measurements cannot properly reveal the influence of radiation. Based on the shape of the P-E hysteresis, leakage current density, and dielectric loss, it has been suggested that radiation does not affect the ferroelectricity in HfO_2 [11]. Similarly, our conventional P-V hysteresis analysis did not reveal any significant difference resulting from the gamma-ray radiation for as-grown specimens, as shown in Fig. 1. However, as shown in Fig. 3, the dynamic analysis of the characteristic switching time observed in the ferroelectric switching dynamics revealed a clear conditional influence of the ferroelectric character, indicated by a change in the characteristic switching time and broadening of its distribution.

For the $Hf_{0.5}Zr_{0.5}O_2$ film in the pristine state, the random orientation of domains with various internal bias fields generates the contracted hysteresis shape of pristine cases, in contrast to that of woken-up cells [29-31]. This explanation is evidenced by comparing the dashed and solid lines in Fig. 1(c). Local defects in the film, such as oxygen vacancies, can pin pristine domain walls and hinder their

movement [22]. Apart from local defects, newly generated defects from irradiation can also pin the domain walls [32]. Thus, a similar shape of hysteresis from electrical measurements can be obtained for nonirradiated and irradiated pristine cases. When the cells are exposed to electric field cycling for the wake-up process, local and radiation-induced defects become redistributed in the films, and depinning of ferroelectric domains occurs [17, 33]. Thus, increased remnant polarization values clarify our results from the experiment, as shown in Figs. 1(c) and (f).

Dissimilar results for irradiated/woken-up cells and woken-up/irradiated cells can be explained by the difference in the distribution of local and radiation-induced defects. As described above, the wake-up process with electric field cycling causes redistribution of defects and domain depinning [17, 33]. However, when the film is irradiated after being woken up, defects from radiation are not diffused in the film. They are affected by alignment of domains shortly after the wake-up and hysteresis measurement. Since the final direction of the electric field after measurement was downward (positive on the top electrode), the orientation of most ferroelectric domains follows the direction, leading charged mobile defects to be asymmetrically distributed. It has been reported that the asymmetric distribution of trapped charges at defect sites near interfaces is influenced by the former direction of domain alignments, which gives rise to a coercive voltage shift toward a negative voltage [34, 35]. Therefore, the hysteresis imprint in Figs. 2(d) and 2(e) can also be attributed to domain wall pinning and the blocking of former domains due to defects [36].

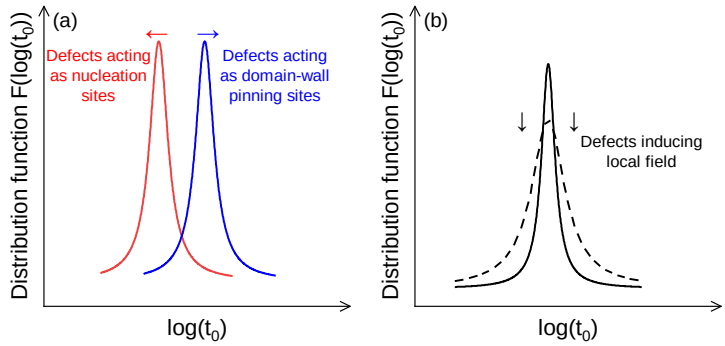

Fig. 4. Schematics describing the effects of defects on the Lorentzian distribution function of switching time. (a) Variation in the characteristic switching time and location of the distribution function based on the role of defects as nucleation sites or domain-wall pinning sites. (b) Variation of broadness of distribution function due to induced local field by defects.

IV. Conclusion

In summary, we have investigated the effect of gamma-ray irradiation on MFM $Hf_{0.5}Zr_{0.5}O_2$ thin films considering their comprehensive application in a radiation environment. The pristine $Hf_{0.5}Zr_{0.5}O_2$ thin film exhibited strong irradiation tolerance against gamma-rays, supporting studies claiming its firmness under radiation. When the $Hf_{0.5}Zr_{0.5}O_2$ thin film was exposed to electric field cycling before irradiation, however, its ferroelectricity demonstrated clear degradation, a coercive voltage shift and reduced remnant polarization values. Radiation-induced defects such as electron-hole pairs and oxygen vacancies can account for this outcome. This explanation is supported by the switching dynamics of $Hf_{0.5}Zr_{0.5}O_2$ after irradiation: faster switching and broadened distribution due to defects acting as nucleation sites and giving rise to local fields, respectively. Thus, the stability of ferroelectric $Hf_{0.5}Zr_{0.5}O_2$ under high-energy gamma-ray irradiation must be reconsidered given the significance of the wake-up effect.

References

[1] T. S. Böscke, J. Müller, D. Bräuhaus, U. Schröder, U. Böttger, Ferroelectricity in hafnium oxide thin films. *Applied Physics Letters*, 2011. **99**(10): p. 102903.

[2] M. Park, Y. Lee, T. Mikolajick, U. Schroeder, C. Hwang, Review and perspective on ferroelectric HfO_2-based thin films for memory applications. *MRS Communications*, 2018. **8**(3): p. 795-808.

[3] T. Mikolajick, S. Slesazeck, M. Park, U. Schroeder, Ferroelectric hafnium oxide for ferroelectric random-access memories and ferroelectric field-effect transistors. *MRS Bulletin*, 2018. **43**(5): p. 340-346.

[4] J. Müller, P. Polakowski, S. Mueller, T. Mikolajick, Ferroelectric hafnium oxide based materials and devices: Assessment of current status and future prospects. *ECS Journal of Solid State Science and Technology*, 2015. **4**(5): p. N30.

[5] T. Shimizu, K. Katayama, T. Kiguchi, A. Akama, T. J. Konno, O. Sakata, H. Funakubo, The demonstration of significant ferroelectricity in epitaxial Y-doped HfO_2 film. *Scientific reports*, 2016. **6**(1): p. 1-8.

[6] J. F. Ihlefeld, D. T. Harris, R. Keech, J. L. Jones, J. P. Maria, S. Trolier-McKinstry, Scaling effects in perovskite ferroelectrics: fundamental limits and process-structure-property relations. *Journal of the American Ceramic Society*, 2016. **99**(8): p. 2537-2557.

[7] D. Das, A. I. Khan, Ferroelectricity in CMOS-Compatible Hafnium Oxides: Reviving the ferroelectric field-effect transistor technology. *IEEE Nanotechnology Magazine*, 2021. **15**(5): p. 20-32.

[8] S. S. Cheema, D. Kwon, N. Shanker, R. Dos Reis, S. Hsu, J. Xiao, H. Zhang, R. Wagner, A. Datar, M. R. McCarter, Enhanced ferroelectricity in ultrathin films grown directly on silicon. *Nature*, 2020. **580**(7804): p. 478-482.

[9] M. Trentzsch, S. Flachowsky, R. Richter, J. Paul, B. Reimer, D. Utess, S. Jansen, H. Mulaosmanovic, S. Müller, S. Slesazeck, A 28nm HKMG super low power embedded NVM technology based on ferroelectric FETs. *2016 IEEE International Electron Devices Meeting (IEDM)*, 2016: p. 11.5.1-11.5.4.

[10] H. Lee, M. Lee, K. Lee, J. Jo, H. Yang, Y. Kim, S. C. Chae, U. Waghmare, J. H. Lee, Scale-free ferroelectricity induced by flat phonon bands in HfO_2. *Science*, 2020. **369**(6509): p. 1343-1347.

[11] Q. Sun, J. Liao, Q. Peng, B. Zeng, J. Jiang, Y. Luo, M. Liao, L. Yin, Y. Zhou, Total ionizing dose effects of ^{60}Co γ-rays radiation on $Hf_xZr_{1-x}O_2$ ferroelectric thin film capacitors. *Journal of Materials Science: Materials in Electronics*, 2020. **31**(3): p. 2049-2056.

[12] W. Zhang, G. Li, X. Long, L. Cui, M. Tang, Y. Xiao, S. Yan, Y. Li, W. Zhao, A comparative study of the γ-ray radiation effect on Zr-doped and Al-doped HfO_2-based ferroelectric memory. *physica status solidi (b)*, 2020. **257**(5): p. 1900736.

[13] K. Chen, Y. Tsai, Y. Wu, Ionizing radiation effect on memory characteristics for HfO_2-based ferroelectric field-effect transistors. *IEEE Electron Device Letters*, 2019. **40**(9): p. 1370-1373.

[14] N. Manikanthababu, N. Arun, M. Dhanunjaya, V. Saikiran, S. Nageswara Rao, A. Pathak, Synthesis, characterization and radiation damage studies of high-k dielectric (HfO_2) films for MOS device applications. *Radiation*

Effects and Defects in Solids, 2015. **170**(3): p. 207-217.

[15] M. Ding, X. Liu, Damage effect of hafnium oxide gate dielectric based metal–oxide–semiconductor structure under gamma-ray irradiation. *AIP Advances*, 2021. **11**(6): p. 065304.

[16] M. Song, K. Lee, J. Choi, K. Lee, S. Chae, Local field inhomogeneity and ferroelectric switching dynamics in $Hf_{1-x}Zr_xO_2$ thin films. *Physical Review Materials*, 2021. **5**(11): p. 114408.

[17] P. Jiang, Q. Luo, X. Xu, T. Gong, P. Yuan, Y. Wang, Z. Gao, W. Wei, L. Tai, H. Lv, Wake-up effect in HfO_2-based ferroelectric films. *Advanced Electronic Materials*, 2021. **7**(1): p. 2000728.

[18] A. K. Tagantsev, I. Stolichnov, N. Setter, J. S. Cross, M. Tsukada, Non-Kolmogorov-Avrami switching kinetics in ferroelectric thin films. *Physical Review B*, 2002. **66**(21): p. 214109.

[19] J. Jo, H. Han, J. Yoon, T. Song, S. Kim, T. Noh, Domain switching kinetics in disordered ferroelectric thin films. *Physical review letters*, 2007. **99**(26): p. 267602.

[20] T. Y. Lee, K. Lee, H. H. Lim, M. S. Song, S. M. Yang, H. K. Yoo, D. I. Suh, Z. Zhu, A. Yoon, M. R. MacDonald, Ferroelectric polarization-switching dynamics and wake-up effect in Si-doped HfO_2. *ACS applied materials & interfaces*, 2018. **11**(3): p. 3142-3149.

[21] S. M. Yang, J. Yoon, T. W. Noh, Nanoscale studies of defect-mediated polarization switching dynamics in ferroelectric thin film capacitors. *Current Applied Physics*, 2011. **11**(5): p. 1111-1125.

[22] Y. Kim, H. Han, I. Vrejoiu, W. Lee, D. Hesse, M. Alexe, Origins of domain wall pinning in ferroelectric nanocapacitors. *Nano Convergence*, 2014. **1**(1):

p. 1-6.

[23] T. Yang, V. Gopalan, P. Swart, U. Mohideen, Direct observation of pinning and bowing of a single ferroelectric domain wall. *Physical review letters*, 1999. **82**(20): p. 4106.

[24] P. Gao, C. T. Nelson, J. R. Jokisaari, S. Baek, C. W. Bark, Y. Zhang, E. Wang, D. G. Schlom, C. Eom, X. Pan, Revealing the role of defects in ferroelectric switching with atomic resolution. *Nature communications*, 2011. **2**(1): p. 1-6.

[25] S. Kaya, A. Jaksic, E. Yilmaz, Co-60 gamma irradiation effects on electrical characteristics of HfO_2 MOSFETs and specification of basic radiation-induced degradation mechanism. *Radiation Physics and Chemistry*, 2018. **149**: p. 7-13.

[26] J. Shi, J. Wang, X. Wang, X. Yu, M. Li, X. Zhang, J. Xue, S. Peng, Radiation-induced charge trapping in Si-MOS capacitors with HfO_2/SiO_2 gate dielectrics. *Nuclear Instruments and Methods in Physics Research Section B: Beam Interactions with Materials and Atoms*, 2020. **479**: p. 150-156.

[27] M. Ding, Y. Cheng, X. Liu, X. Li, Total dose response of hafnium oxide based metal-oxide-semiconductor structure under gamma-ray irradiation. *IEEE Transactions on Dielectrics and Electrical Insulation*, 2014. **21**(4): p. 1792-1800.

[28] C. Zhao, S. Taylor, M. Werner, P. Chalker, R. Potter, J. Gaskell, A. Jones, High-k materials and their response to gamma ray radiation. *Journal of Vacuum Science & Technology B: Microelectronics and Nanometer Structures Processing, Measurement, and Phenomena*, 2009. **27**(1): p. 411-415.

[29] F. Fengler, M. H. Park, T. Schenk, M. Pešić, U. Schroeder, *Field Cycling Behavior of Ferroelectric HfO_2-Based Capacitors*, in *Ferroelectricity in Doped Hafnium Oxide: Materials, Properties and Devices*. 2019, Elsevier. p. 381-398.

[30] T. Schenk, M. Hoffmann, J. Ocker, M. Pešić, T. Mikolajick, U. Schroeder, Complex internal bias fields in ferroelectric hafnium oxide. *ACS applied materials & interfaces*, 2015. **7**(36): p. 20224-20233.

[31] H. J. Kim, M. H. Park, Y. J. Kim, Y. H. Lee, T. Moon, K. Do Kim, S. D. Hyun, C. S. Hwang, A study on the wake-up effect of ferroelectric $Hf_{0.5}Zr_{0.5}O_2$ films by pulse-switching measurement. *Nanoscale*, 2016. **8**(3): p. 1383-1389.

[32] S. A. Yang, B. H. Kim, M. K. Lee, G. J. Lee, N. Lee, S. D. Bu, Gamma-ray irradiation effects on electrical properties of ferroelectric $PbTiO_3$ and $Pb(Zr_{0.52}Ti_{0.48})O_3$ thin films. *Thin Solid Films*, 2014. **562**: p. 185-189.

[33] F. P. Fengler, M. Pešić, S. Starschich, T. Schneller, C. Künneth, U. Böttger, H. Mulaosmanovic, T. Schenk, M. H. Park, R. Nigon, Domain pinning: Comparison of hafnia and PZT based ferroelectrics. *Advanced Electronic Materials*, 2017. **3**(4): p. 1600505.

[34] H. N. Al-Shareef, D. Dimos, W. Warren, B. Tuttle, Voltage offsets and imprint mechanism in $SrBi_2Ta_2O_9$ thin films. *Journal of Applied Physics*, 1996. **80**(8): p. 4573-4577.

[35] W. Warren, D. Dimos, G. Pike, B. Tuttle, M. Raymond, R. Ramesh, J. Evans Jr, Voltage shifts and imprint in ferroelectric capacitors. *Applied Physics Letters*, 1995. **67**(6): p. 866-868.

[36] T. Rojac, M. Kosec, B. Budic, N. Setter, D. Damjanovic, Strong ferroelectric

domain-wall pinning in $BiFeO_3$ ceramics. *Journal of Applied Physics*, 2010. **108**(7): p. 074107.

Abstract in Korean

이 논문에서는 ^{60}Co 감마선 조사에 의한 $Hf_{0.5}Zr_{0.5}O_2$ 박막의 강유전 안정성과 스위칭 동역학에 대하여 연구하였다. 전기적인 측정 혹은 wake-up이 이루어지지 않은 $Hf_{0.5}Zr_{0.5}O_2$ 박막의 경우 감마선 조사 이후에도 영향을 받지 않고 안정적인 강유전 성질을 보였다. 하지만 wake-up 과정을 거친 $Hf_{0.5}Zr_{0.5}O_2$ 박막은 감마선 조사 후에 이력 곡선에 나타난 잔류 분극과 보자 전압의 변화를 통하여 저하된 강유전 성질을 보였다. 나아가 스위칭 동역학 분석을 통하여 방사선 조사량이 많을수록 스위칭 시간이 빨라지고 스위칭 시간에 대한 분포가 넓게 퍼진다는 사실을 알게 되었으며, 이는 기존에 알려진 wake-up 과정과 상반된 결과를 보여준다. 최종적으로 강유전 $Hf_{0.5}Zr_{0.5}O_2$의 wake-up 과정과 감마선 조사에 의한 안정성 사이의 관계를 강유전 도메인의 배열과 결함의 메커니즘, 즉 결함 전하들의 재분포와 트래핑을 통하여 논의하였다.

주요어 : 강유전성, $Hf_{0.5}Zr_{0.5}O_2$, 감마선, wake-up, 스위칭 동역학, 결함

학 번 : 2020-27908